HOKKAIDO UNIVERSITY

Title	Transition from equilibrium to nonequilibrium combustion of premixed burner flame by microwave irradiation
Author(s)	Sasaki, Koichi; Shinohara, Koji
Citation	Journal of Physics D: Applied Physics, 45(45), 455202 https://doi.org/10.1088/0022-3727/45/45/455202
Issue Date	2012-11-14
Doc URL	https://hdl.handle.net/2115/50791
Rights	This is an author-created, un-copyedited version of an article accepted for publication in Journal of Physics D: Applied Physics. IOP Publishing Ltd is not responsible for any errors or omissions in this version of the manuscript or any version derived from it. The definitive publisher authenticated version is available online at 10.1088/0022-3727/45/45/455202.
Type	journal article
File Information	JoPD45-45_455202.pdf

Hokkaido University Collection of Scholarly and Academic Papers : HUSCAP

Transition from equilibrium to nonequilibrium combustion of premixed burner flame by microwave irradiation

Koichi Sasaki[1] **and Koji Shinohara**[2]

[1]Division of Quantum Science and Engineering, Hokkaido University, Kita 13, Nishi 8, Kita-ku, Sapporo 080-8628, Japan

[2]Department of Electrical Engineering and Computer Science, Nagoya University, Furo-cho, Chikusa-ku, Nagoya 464-8603, Japan

E-mail: sasaki@qe.eng.hokudai.ac.jp

Abstract.

We found that the burning velocity in premixed burner flame was enhanced by heated electrons in the flame. The electron heating was realized by irradiating microwave power onto the flame, and was confirmed by observing optical emission intensity of molecular nitrogen at the second positive system. Since the increase of the observed gas temperature was negligible, the enhancement of the burning velocity can be attributed to the nonequilibrium combustion chemistry which is driven by energetic electrons. We examined the time constants for the transition between equilibrium and nonequilibrium combustion states by irradiating pulsed microwave power. As a result, we found $> 2 \times 10^4$ s^{-1} for the frequency of electron heating, $\sim 1 \times 10^3$ s^{-1} for the loss frequency of heated electrons, and $\sim (0.5 - 1) \times 10^3$ s^{-1} for the loss frequencies of OH and CH radicals.

1. Introduction

The development of novel combustion technologies attracts much interest of many researchers. A driving force is the demand to avoid global warming due to the greenhouse effect since more than 80% of fossil fuels are consumed by combustion. Recently, plasma-assisted combustion has been investigated as an innovative technology [1], which is expected to be useful for combustion in a lean-fuel condition [2, 3] and in a speedy flow [4–6]. In addition, it is considered that plasmas can be utilized for improving the ignition characteristics [7–11] and the stability of flames [12, 13]. Since the ignition in a lean-fuel condition of an automobile engine results in the reduction in the consumption of fossil fuels, plasma-assisted combustion could contribute greatly to the avoidance of global warming.

The principal concept of plasma-assisted combustion is the shift of combustion chemistry from the conventional one in thermodynamic equilibrium to a nonequilibrium state [14, 15]. The nonequilibrium combustion is realized with the help of energetic electrons. In general, the temperature (the mean energy) of electrons in a nonequilibrium plasma is much higher than the gas temperature, and chemical reactions in the nonequilibrium plasma is driven by electron impact dissociation and excitation of neutral species [16–18]. In the case of combustion chemistry, for example, the production of OH radicals [19, 20] is expected due to electron impact dissociation of H_2O. The combustion of biomass fuels with a large amount of H_2O is difficult because of the endoergic nature, while the combustion can be activated if H_2O is converted into OH radicals by electron impact dissociation. The increase in the gas temperature is not favorable as an effect of the plasma, since a higher combustion temperature results in the oxidation of nitrogen and more emission of toxic NO_x.

Various techniques have been developed for superposing plasmas onto combustion flames [21–28]. In a previous paper [29], we reported a fundamental experiment where a premixed burner flame was irradiated by microwave power. The microwave-induced discharge (the discharge sustained by the microwave power) was avoided in this experiment. The enhancement of the burning velocity in the flame was estimated from the fact that a shortened flame length was observed when the flame was irradiated by the microwave power. Since negligible increase in the gas temperature was observed by the microwave irradiation, we surmised that the enhancement of the burning velocity was realized by the effect of electron heating in the flame.

In this paper, we report an experimental evidence of the electron heating in a premixed burner flame irradiated by microwave power. In addition, we examined the transient phenomena observed in the premixed burner flame irradiated by pulsed microwave power. We evaluated the time constants of electron heating and particle densities. The results give us useful insights for understanding the transition between equilibrium and nonequilibrium combustion chemistries.

2. Experiment

The experimental apparatus has been reported previously [29]. As shown in Fig. 1(a), microwave power at a frequency of 2.45 GHz was generated using a magnetron source, and was transmitted using a WRJ-2 rectangular waveguide system. The magnetron source was connected to an isolator, a power monitor, and an EH tuner. After the EH tuner, the size of the waveguide was reduced to the WST-AD type. The WST-AD waveguide had holes on the H- and E-planes. A premixed burner was attached on the bottom-side H-plane, as shown in Fig. 1(b). The hole on the top-side H-plane was connected to viewing pipes which were used for avoiding the leak of the microwave power and for observing the top part of the flame. The bottom part of the flame was observed through another viewing pipes (with diameters of 10 mm) attached to the holes on the E-planes. A plunger was placed at the end of the waveguide system to obtain the maximum electric field strength of the standing wave at the flame position. As shown in Fig. 1(a), conventional optical emission spectroscopy was performed through the bottom-side viewing pipe using a spectrograph with a focal length of 50 cm combined with a charge-coupled device camera with a gated image intensifier (ICCD camera). Another ICCD camera was used for capturing the picture of the top part of the flame.

The structure of the nozzles of the premixed burner is schematically shown in Fig. 1(c). The premixed burner was operated using the mixture of methane and dry air with flow rates of 0.5 and 5 l/min, respectively. The gas flow rates were adjusted using mass flow controllers. The mass flow controllers were connected to the burner via a gas mixing system. The burner had two gas-feed lines. One was the direct connection line between the gas mixing system and the main nozzle with a diameter of 2 mm. The other was the connection line to eight sub-nozzles which surrounded the main nozzle. The diameters of the sub-nozzles were 1.7 mm. The sub-nozzles were connected to the main nozzle via two orifices with diameters of 0.8 mm. Considering the geometries and the structures of the gas-feed lines, it was estimated that 72% of the total gas supplied using the mass flow controllers passed through the main nozzle. In accordance with this, the flow speed of the gas at the main nozzle was evaluated as 20.9 m/s. A flame with a length of 44 mm passed through the WST-AD waveguide at the above gas-feed condition.

3. Results and discussion

3.1. Enhancement of burning velocity

The enhancement of the burning velocity by the irradiation of the microwave power has been reported in a previous paper [29], and we summarize the experimental results briefly here. We observed the shortening of the flame length from 44 mm to 37 mm when we irradiated a microwave power of 300 W onto the flame. When we ignore the attachments of the burner and the viewing pipes, the electric field corresponding to 300 W in the WST-AD waveguide was 302 V/cm at the position of the flame. In addition,

we observed the increase in the optical emission intensity in the flame. The shortened flame length indicates the increase in the burning velocity in the flame. According to a simplified analysis based on the shape of the flame, it was evaluated that the burning velocity in the premixed burner flame increased with an enhancement factor of 1.19 by irradiating the microwave power of 300 W. It is noted here that the entire microwave power of 300 W was not absorbed by the flame, even though the fact that negligible amount of reflected microwave power was observed at the power monitor in Fig. 1(a). This was because we observed significant heating of the microwave components by the microwave power itself.

3.2. Gas temperature

As also reported in a previous paper [29], we examined the change in gas temperature by observing the optical emission spectra of CH and OH radicals. We evaluated the rotational temperatures of CH and OH by fitting the optical emission spectra using spectral simulations [30]. As a result, we evaluated 2150 ± 40 and 2900 ± 50 K for the rotational temperatures of CH and OH, respectively, when the flame was irradiated by no microwave power. The rotational temperatures in the presence of the microwave power of 300 W were 2150 ± 50 and 2880 ± 40 K for CH and OH, respectively. Therefore, the observed gas heating by the microwave power is negligible. On the other hand, if the combustion of the flame is in the thermodynamic equilibrium, the enhancement factor of 1.19 for the burning velocity needs an increase in the gas temperature with a factor of 1.04 (the increase of $100 - 150$ K). Therefore, it can be said that the enhancement of the burning velocity was not caused by the increase in the gas temperature. These experimental results are different from those observed by Stockman *et al* [31]. They observed both the enhancement of the burning velocity and the increase in the gas temperature in a premixed burner flame irradiated by a microwave power of 1.3 kW. One of the reasons of the negligible gas heating in our experiment may lie in the weak microwave power. In our experiment, only a small fraction of the microwave power of 300 W was probably absorbed by the flame.

3.3. Evidence of electron heating

Because of the enhancement of the burning velocity without heating the gas temperature, we expected nonequilibrium combustion that was driven by energetic electrons. The evidence of electron heating was obtained by observing the optical emission intensity of molecular nitrogen at the second positive [32]. Figure 2(a) shows an optical emission spectrum in the wavelength range corresponding to the second positive system, which was observed from the bottom part of the flame when no microwave power was irradiated. As shown in the figure, the optical emission intensity of molecular nitrogen was negligible in the normal flame. It is reasonable since the normal flame is in the thermodynamic equilibrium at a temperature of 2100 K (the rotational temperature of CH) or 2900 K (the rotational temperature of OH), while the energy of $N_2(C^3\Pi_u)$,

which is the upper electronic state of the second positive system, is $\sim$ 11 eV. In contrast, as shown in Fig. 2(b), we observed a clear spectrum of the second positive system of molecular nitrogen when we irradiated the microwave power of 300 W. It is noted that molecular nitrogen is almost inert in the methane/air combustion [33–35]. In addition, it was shown that the gas temperature was unchanged by the microwave irradiation. Hence, the clear optical emission spectrum of the second positive system shown in Fig. 2(b) suggests the production of $N_2(C^3\Pi_u)$ by electron impact excitation. In other words, Fig. 2(b) indicates the existence of a considerable amount of electrons with energies higher than $\sim$ 11 eV, and is an evidence of electron heating in the flame by the microwave irradiation.

From the quantitative point of view, however, it is difficult to explain the remarkable optical emission intensity of the second positive system observed experimentally. The rate coefficient for electron impact excitation from $N_2(X^1\Sigma_g^+)$ to $N_2(C^3\Pi_u)$ is negligibly small at the experimental electric field of 302 V/cm. The electric field of 302 V/cm, which corresponds to a reduced electric field of $\sim$ 10 Td, was calculated by ignoring the attachments of the burner and the viewing pipes. As will be reported in a separate paper, in which we will discuss the kinetics of electrons, we estimate that a reduced electric field of $\sim$ 60 Td is necessary to explain the optical emission intensity of the second positive system. At the moment, we guess localized strong electric field at the edges of the burner nozzles and the holes on the inner surface of the waveguide. We will continue further investigation to obtain more quantitative understanding of the optical emission intensity of the second positive system.

3.4. Time constants in transition between equilibrium and nonequilibrium combustion states

The time constant in the transition to the nonequilibrium combustion state gives us a useful insight for understanding the nonequilibrium combustion chemistry. To examine the time constant, we used a pulsed microwave power with a duration of 2 ms and a repetition rate of 250 Hz. The instantaneous microwave power was 300 W, and the rise and decay time constants of the microwave power were less than $\sim$ 1 μs. We observed the optical emission spectrum from the bottom part of the flame. The temporal variation of the optical emission spectrum was obtained by operating the ICCD camera in the gate mode with a duration of 50 μs and by changing the delay time between the rise time of the microwave power and the trigger to the gate of the ICCD camera.

Figure 3 shows the temporal variation of the optical emission intensity of molecular nitrogen at the second positive system. As described in the previous section, the optical emission intensity at the second positive system before the irradiation of the microwave power was negligible. The optical emission intensity increased gradually, as shown in Fig. 3, after the microwave power was switched on. The temporal evolution was approximated by an exponential function with a time constant of 0.35 ms. On the other hand, a sudden decrease in the optical emission intensity at the second positive system

was observed when the microwave power was switched off. The decay time constant was shorter than the step of the delay time (50 μs). The negative optical emission intensity at around $\sim$ 2.5 ms was due to the difficulty in the subtraction of the continuum optical emission intensity, which was observed in the wavelength range of the second positive system as shown in Fig. 2.

Figures 4(a) and 4(b) show the temporal variations of the optical emission intensities of OH ($A^2\Sigma^+ \rightarrow X^2\Pi$) and CH ($A^2\Delta \rightarrow X^2\Pi$), respectively. The temporal evolutions of the optical emission intensities of OH and CH, which were observed after we switched on the microwave power, were approximated by exponential functions. The rise time constants were 0.35 and 0.4 ms for OH and CH, respectively. On the other hand, the decay time constants of the optical emission intensities of both OH and CH were 0.35 ms.

The temporal variation of the continuum optical emission intensity at a wavelength of 430 nm is shown in Fig. 5. The rise and decay curves were approximated by exponential functions with a time constant of 0.5 ms. We also examined the temporal variations of the continuum optical emission intensities at wavelengths of 310 and 340 nm. The result was that the same time constant of 0.5 ms were observed for the rise and the decay in the temporal variations of the continuum optical emission intensities at 310 and 340 nm.

The residence time of gas in the bottom-side observation region was estimated to be 0.48 ms, based on the length (10 mm) of the observation region and the flow speed of the gas (20.9 m/s). The rise and decay time constants of 0.5 ms, which were observed for the continuum optical emission intensities as shown in Fig. 5, agreed well with the residence time of gas. It can be reasonably explained since it is widely understood that the continuum optical emissions in hydrocarbon-based combustion flames originates from HCO (310 and 340 nm) [36] and CO-O recombination (430 nm) [37], and the intensity of the continuum optical emission is related to the amount of reaction products. On the other hand, it is considered that the decay time constant of < 0.05 ms shown in Fig. 3 represents the cooling time constant of electron energy. The cooling time constant of electron energy may be equal to the heating time constant. Hence, the rise time constant of 0.35 ms for the optical emission intensity of the second positive system of molecular nitrogen may represent the lifetime of heated electrons. The loss process of heated electrons comprises of transport and gas-phase reactions. The transport is the flow with gas, and the loss frequency due to the gas flow is $\sim 2 \times 10^3$ s^{-1} (corresponding to the gas residence time of 0.48 ms). Therefore, to explain the rise time constant of 0.35 ms shown in Fig. 3, it is necessary to assume a gas-phase process with a frequency of $\sim 1 \times 10^3$ s^{-1}. The details of the gas-phase process of electrons have not yet been fully understood, and we will discuss the kinetics of electrons in a separate paper. The rise and decay time constants of the optical emission intensities of OH and CH are also determined by the transport and gas-phase reactions. According to the rise and decay time constants of 0.35–0.4 ms shown in Fig. 4, the frequencies of gas-phase reactions of OH and CH are estimated to be $\sim (0.5 - 1) \times 10^3$ s^{-1}.

3.5. Transient phenomena observed at the top of flame

We took time-resolved pictures of the top part of the flame after switching on and off the microwave power. In this experiment, we used pulsed microwave power with a duration of 4 ms and a repetition rate of 125 Hz. The instantaneous microwave power was 300 W. The gate width of the ICCD camera was 25 μs, and the temporal variation was obtained by changing the delay time between the rise time of the microwave power and the trigger to the gate of the ICCD camera. No interference filters were placed in front of the camera. We employed the shorter gate width than that for obtaining Figs. 3-5 (50 μs), since the signal intensity was stronger when the ICCD camera was used for capturing the picture of the flame.

Figure 6 shows the pictures of the top part of the flame at various delay times after switching on the microwave power. Figure 6(a) shows the length of the flame in the steady-state condition. As shown in the figure, the transient change at the top part of the flame started with a longer delay time than that at the bottom part. The flame at 0.5 ms after the initiation of the microwave power kept roughly the same length as that of the steady-state flame, as shown in Fig. 6(b). The flame started shortening at $\sim$ 1 ms, as shown in Fig. 6(c). The delay in the transient change between the top and bottom parts of the flame is attributed to the flow speed of the gas. We could not observe the top part of the flame after 1.5 ms, as shown in Figs. 6(d) and 6(e), since it was hidden by the vertical observation pipe. As reported in a previous paper [29], the shortened flame lengths indicates the enhancement of the burning velocity.

We observed more interesting transient phenomena at the top part of the flame, when we switched off the microwave power. We observed shortened flame length even at 1 ms after the termination of the microwave power, as shown in Fig. 7(a). The sudden stretch of the flame was observed at 1.8 ms after the termination of the microwave power, as shown in Fig. 7(b). The stretch of the flame did not monotonically continue. As shown in Figs. 7(d)–7(o), we observed the oscillation of the flame length with a repetition period of $\sim$ 0.08 ms. The oscillation of the flame length resulted in the phenomenon which appeared like the propagation of bullets along the vertical direction. The propagation speed of the bullets was roughly consistent with the flow speed of gas. The oscillation of the flame length began to fall at $\sim$ 2.6 ms after the termination of the microwave power, as shown in Fig. 7(p). The flame length changed back to the original at $\sim$ 3 ms, as shown in Figs. 7(s) and 7(t).

The transient change in the flame length shown in Figs. 6 and 7 gives us a helpful insight into the transition between the equilibrium and nonequilibrium combustion states. In particular, it is important to note that the flame length that is longer than the original one was observed temporarily when we switched off the microwave power. The longer flame length suggests a burning velocity which is slower than that in the normal flame. The elongated flame length was followed by the shortened flame length, or the enhanced burning velocity. The oscillation of the flame length may be explained as follows. The shortened flame length with an enhanced burning velocity is caused by

radicals, which were produced by electron impact processes at the bottom side of the flame. The production of radicals due to electron impact processes stops immediately after the termination of the microwave power because of the rapid electron cooling, as shown in Fig. 3. However, the enhanced combustion chemistry continues through radicals' lifetime. The excessive consumption (or the lower densities) of radicals is caused by the continuously-enhanced combustion chemistry, which resulted in the slower burning velocity than that of the normal flame. The less efficient combustion results reversely in higher densities of radicals, enhanced burning velocity, and shortened flame length. These overshooting phenomena may occur in the middle part of the flame where no microwave power was irradiated. The aforementioned explanation is a speculation which is not supported by experimental evidence. Further investigation is necessary to obtain more reliable understanding on the oscillation of the flame length.

4. Conclusions

In this work, we report an evidence of electron heating in a premixed burner flame by the irradiation of the microwave power. Since no gas heating was observed, the enhancement of the burning velocity by the microwave irradiation is considered to be caused by nonequilibrium combustion chemistry, where energetic electrons play important roles in the production of radicals. In addition, we reported the time constants in the transition between the equilibrium and nonequilibrium combustion states. Exponential variations in the optical emission intensities were observed in the bottom part of the flame, which gave us the knowledge on the time constants of electron heating (cooling), the loss frequency of heated electrons, and the loss frequencies of OH and CH radicals. The time constants observed in the region with the microwave irradiation represent the direct effects of electron heating. On the other hand, more complicated transient phenomena were observed at the top of the flame. The oscillation of the flame length, or the burning velocity, is understood to be a result of overshooting between equilibrium and nonequilibrium combustion chemistries. The experimental results shown in this paper give us useful insights into the transition between the equilibrium and nonequilibrium combustion states.

Acknowledgments

The authors are grateful to H. Akashi for valuable discussion on the kinetics of electrons. This work was supported by Grants-in-Aid for Scientific Research from Japan Society for the Promotion of Science.

References

[1] Starikovskaia S M 2006 *J. Phys. D: Appl. Phys.* **39** R265
[2] Ikeda Y, Nishiyama A, Wachi Y, and Kaneko M 2009 *SAE International* Paper Number 2009-01-1050.

[3] Ikeda Y, Nishiyama A, Katano H, Kaneko M, and Han J 2009 *SAE International* Paper Number 2009-01-1049.

[4] Leonov S B, Yarantsev D A, Napartovich A P, and Kochetov I V 2006 *IEEE Trans. Plasma Sci.* **34** 2514

[5] Esakov I I, Grachev L P, Khodataev K V, Vinogradov V A, and van Wie D M *IEEE Trans. Plasma Sci,* **34** 2497

[6] Leonov S B and Yarantsev D A 2007 *Plasma Sources Sci. Technol.* **16** 132

[7] Pancheshnyi S Y, Lacoste D A, Bourdon A, and Laux C O 2006 *IEEE Trans. Plasma Sci.* **34** 2478

[8] Lou G, Bao A, Nishihara M, Keshav S, Utkin Y G, Rich J W, Lempert W R, and Adamovich I V 2007 *Proc. Combust. Inst.* **31** 3327

[9] Bao A, Utkin Y G, Keshav S, Lou G, and Adamovich I V 2007 *IEEE Trans. Plasma Sci.* **35** 1628

[10] Aleksandrov N L, Kindysheva S V, Kosarev I N, Starikovskaia S M, and Starikovskii A Y 2009 *Proc. Combust. Inst.* **32** 205

[11] Wu L, Lane J, Cernansky N P, Miller D L, Fridman A A, and Starikovskiy A Y 2011 *Proc. Combust. Inst.* **33** 3219

[12] Pilla G, Galley D, Kacoste D A, Lacas F, Veynante D, and Laux C O 2006 *IEEE Trans. Plasma Sci.* **34** 2471

[13] Pham Q L L, Lacoste D A, and Laux C O 2011 *IEEE Trans. Plasma Sci.* **39** 2264

[14] Chintala N, Bao A, Lou G, and Adamovich I V 2006 *Combust. Flame* **144** 744

[15] Adamovich I V, Choi I, Jiang N, Kim J-H, Keshav S, Lempert W R, Mintusov E, Nishihara M, Samimy M, and Uddi M 2009 *Plasma Sources Sci. Tecgnol.* **18** 034018

[16] Uddi M, Jiang N, Mintusov E, Adamovich I V, and Lempert W R 2009 *Proc. Combust. Inst.* **32** 929

[17] Ombrello T, Won S H, Ju Y, and Williams S 2010 *Combust. Flame* **157** 1906

[18] Ombrello T, Won S H, Ju Y, and Williams S 2010 *Combust. Flame 157* 1916

[19] Wu L, Lane J, Cernansky N, Miller D, Fridman A, and Starikovskiy A 2011 *IEEE Trans. Plasma Sci.* **39** 2604

[20] Choi I, Yin Z, Adamovich I V., and Lempert W R 2011 *IEEE Trans. Plasma Sci.* **39** 3288

[21] Kim Y, Ferreri V W, Rosocha L A, Anderson G K, Abbate S, and Kim K-T 2006 *IEEE Trans. Plasma Sci.* **34** 2532

[22] Omebrello T, Ju Y, and Fridman A 2008 *AIAA J.* **46** 2424

[23] Hemawas K W, Wichman I S, Lee T, Grotjohn T A, and Asmussen J 2009 *Rev. Sci. Instrum.* **80** 053507

[24] Korolev Y D, Frants O B, Landl N V, Geyman V. G, Shemyakin I A, Enenko A A, and Matveev I B 2009 *IEEE Trans. Plasma Sci.* **37** 2314

[25] Matveev I B, Matveeva S A, Kirchuk E Y, Serbin S I, and Bazarov V G 2010 *IEEE Trans. Plasma Sci.* **38** 3313

[26] Tang J, Zhao W, and Duan Y 2011 *Plasma Sources Sci. Technol. 20* 045009

[27] Hammack S, Rao X, Lee T, and Carter C 2011 *IEEE Trans. Plasma Sci.* **39** 3300

[28] Schmidt J B and Ganguly B N 2012 *J. Phys. D: Appl. Phys.* **45** 045203

[29] Shinohara K, Takada N, and Sasaki K 2009 *J. Phys. D: Appl. Phys.* **42** 182008

[30] http://www.sri.com/psd/lifbase/

[31] Stockman E S, Zaidi S H, Miles R B, Carter C D, and Ryan M D 2009 *Combust. Flame* **156** 1453

[32] B Pearse R W B and Gaydon A G 1976 *The identification of molecular spectra. Fourth Edition* (Chapman and Hall, London)

[33] Willliams F A 1994 *Combustion Theory, 2nd Ed.* (Benhamin/Cummings, Menlo Park)

[34] Kuo K K 2005 *Principles of Combustion, 2nd Ed.* (Wiley, Hoboken)

[35] Warnatz J, Maas U, and Dibble R W 2006 *Combustion, 4th Ed.* (Springer, Berlin Heidelberg)

[36] Vaidya W M 1934 *Proc. R. Soc. Lond. A* **147** 513

[37] Gaydon A G 1974 *The Scectroscopy of Flame, 2nd Ed.* (Chapman and Hall, London)

Figure captions

Fig. 1 Schematic illustrations of experimental apparatus. (a) Transmission system for microwave, (b) an enlarged illustration of microwave-irradiation part, and (c) the structure of the nozzles.

Fig. 2 Optical emission spectra of the flame in the wavelength range corresponding to the second positive system of molecular nitrogen. (a) and (b) were observed without and with the microwave irradiation, respectively.

Fig. 3 Temporal variation of the optical emission intensity of the second positive system of molecular nitrogen when the flame was irradiated by pulsed microwave power.

Fig. 4 Temporal variations of the optical emission intensities of (a) OH ($A^2\Sigma^+ \rightarrow X^2\Pi$) and (b) CH ($A^2\Delta \rightarrow X^2\Pi$) when the flame was irradiated by pulsed microwave power.

Fig. 5 Temporal variation of the continuum optical emission intensity at a wavelength of 430 nm when the flame was irradiated by pulsed microwave power.

Fig. 6 Snap shots of the top part of the flame at delay times of (a) 0, (b) 0.5, (c) 1, (d) 1.5, and (e) 2 ms after the irradiation of pulsed microwave power.

Fig. 7 Snap shots of the top part of the flame at delay times of (a) 1, (b) 1.8, (c) 1.825, (d) 1.85, (e) 1.875, (f) 1.9, (g) 1.925 (h) 1.95, (i) 1.975, (j) 2 (k) 2.025, (l) 2.05, (m) 2.075, (n) 2.1 (o) 2.125 (p) 2.6, (q) 2.65, (r) 2.7, (s) 3, and (t) 4 ms after the termination of pulsed microwave power.

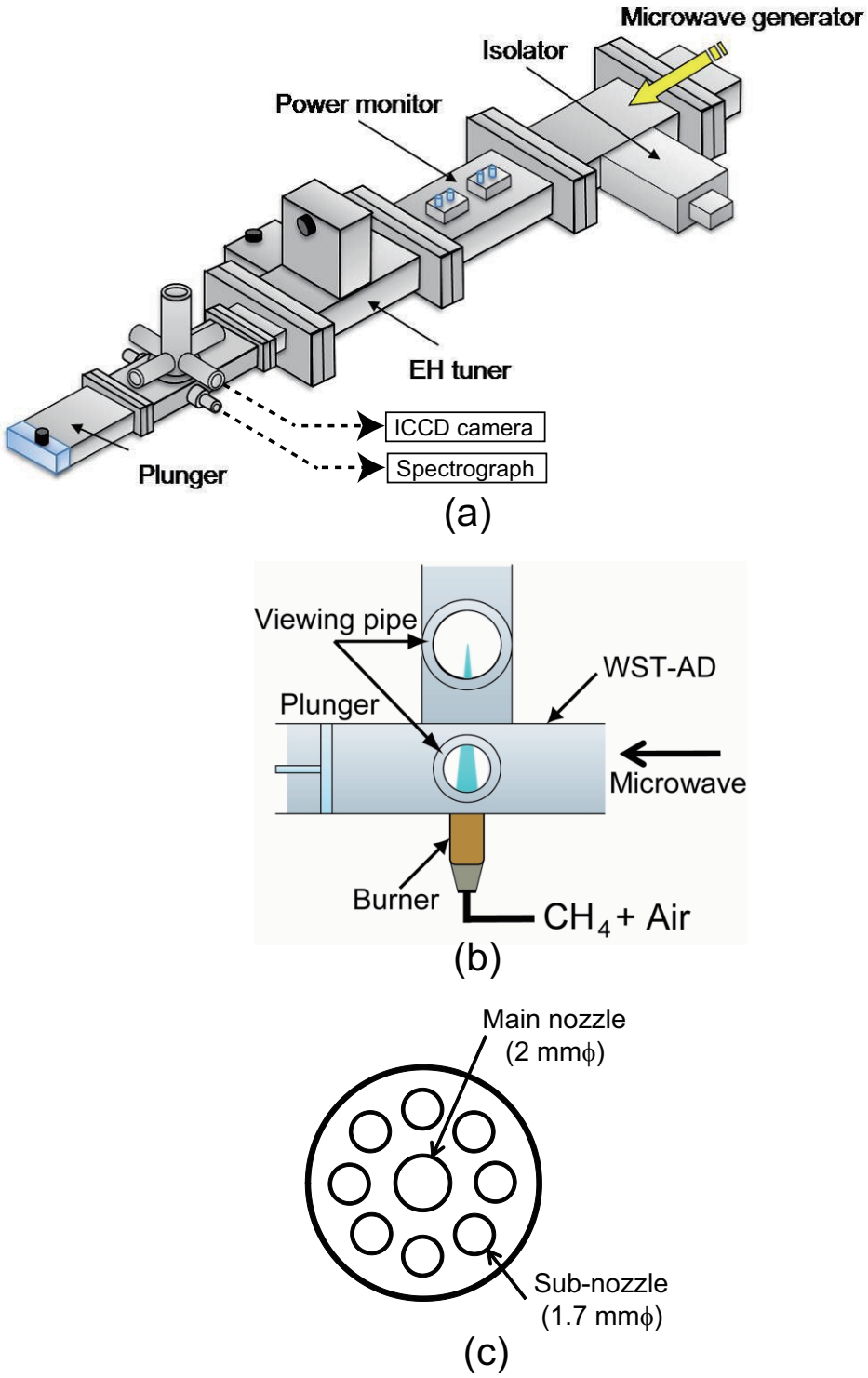

Figure 1. Schematic illustrations of experimental apparatus. (a) Transmission system for microwave, (b) an enlarged illustration of microwave-irradiation part, and (c) the structure of the nozzles.

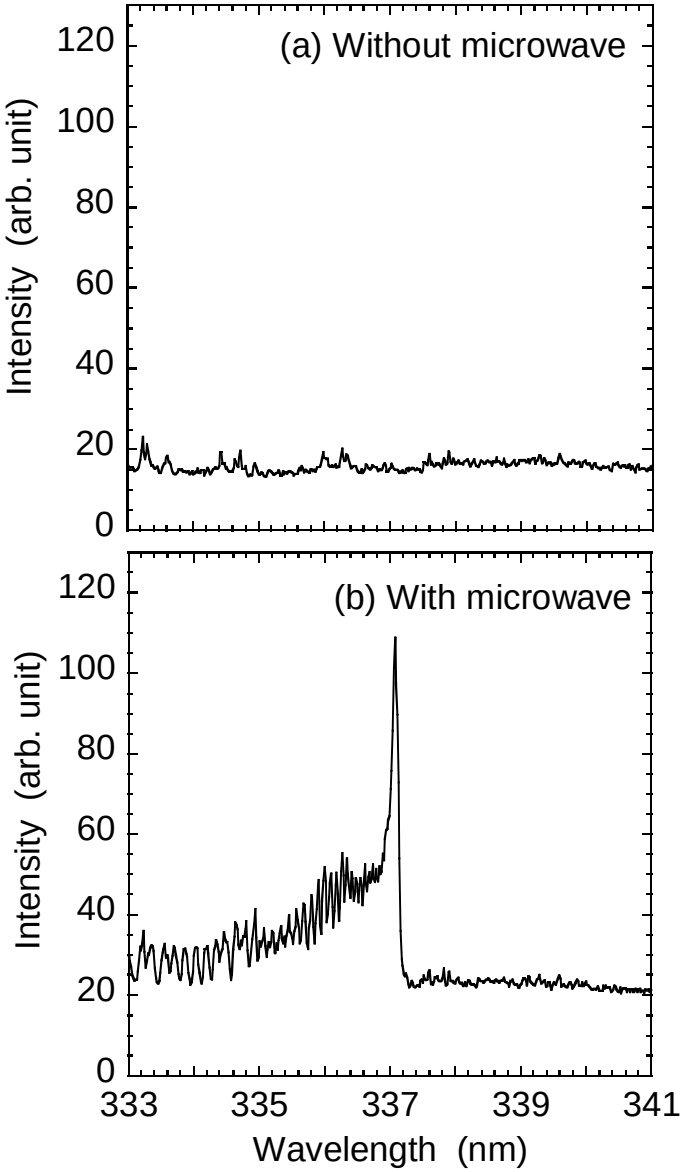

Figure 2. Optical emission spectra of the flame in the wavelength range corresponding to the second positive system of molecular nitrogen. (a) and (b) were observed without and with the microwave irradiation, respectively.

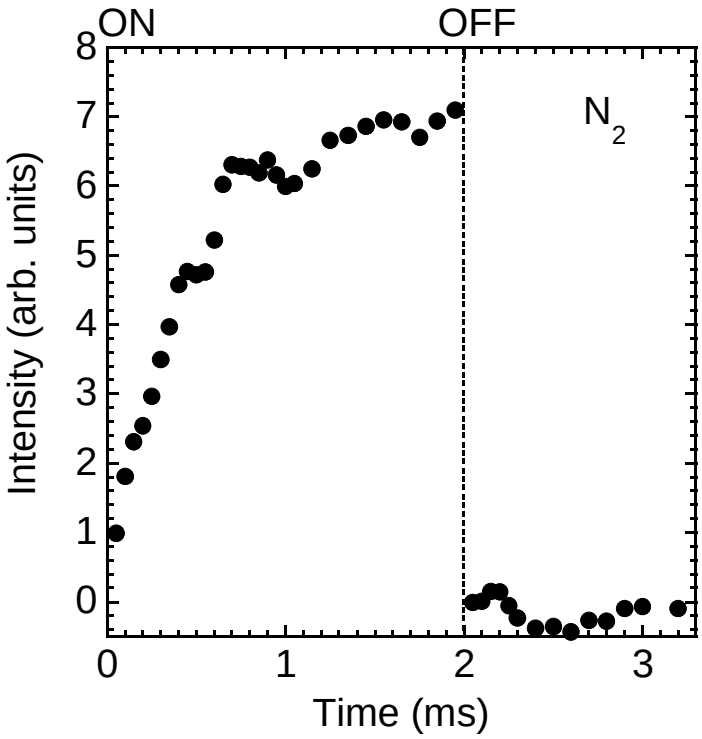

Figure 3. Temporal variation of the optical emission intensity of the second positive system of molecular nitrogen when the flame was irradiated by pulsed microwave power.

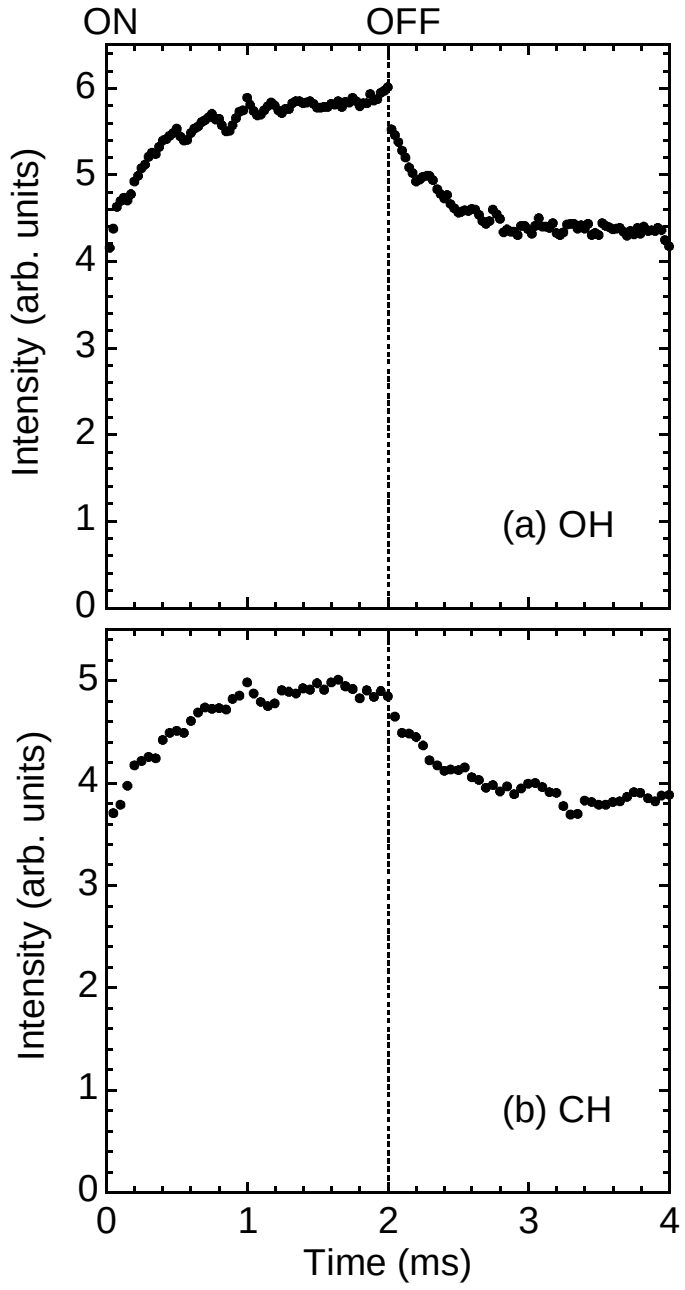

Figure 4. Temporal variations of the optical emission intensities of (a) OH ($A^2\Sigma^+ \rightarrow X^2\Pi$) and (b) CH ($A^2\Delta \rightarrow X^2\Pi$) when the flame was irradiated by pulsed microwave power.

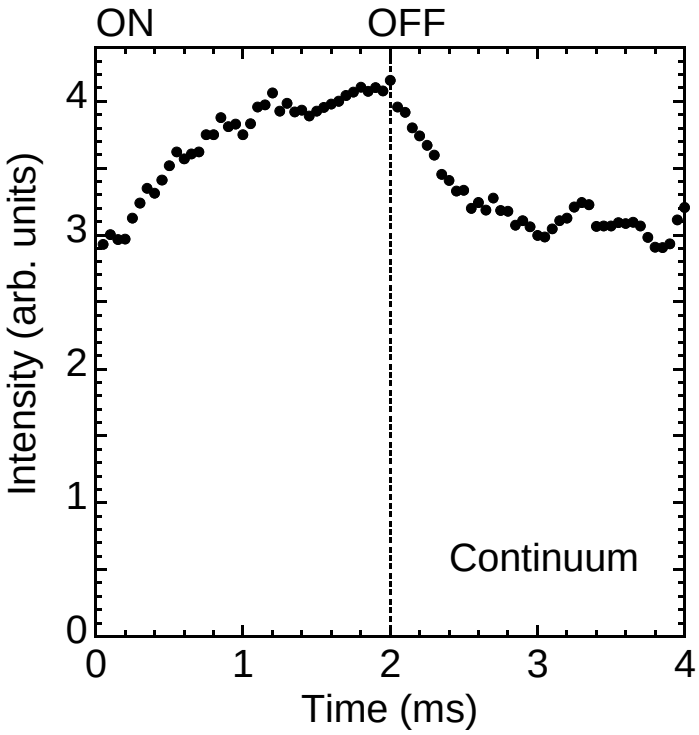

Figure 5. Temporal variation of the continuum optical emission intensity at a wavelength of 430 nm when the flame was irradiated by pulsed microwave power.

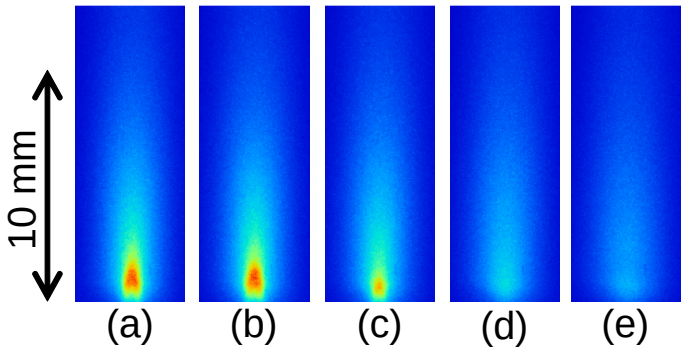

Figure 6. Snap shots of the top part of the flame at delay times of (a) 0, (b) 0.5, (c) 1, (d) 1.5, and (e) 2 ms after the irradiation of pulsed microwave power.

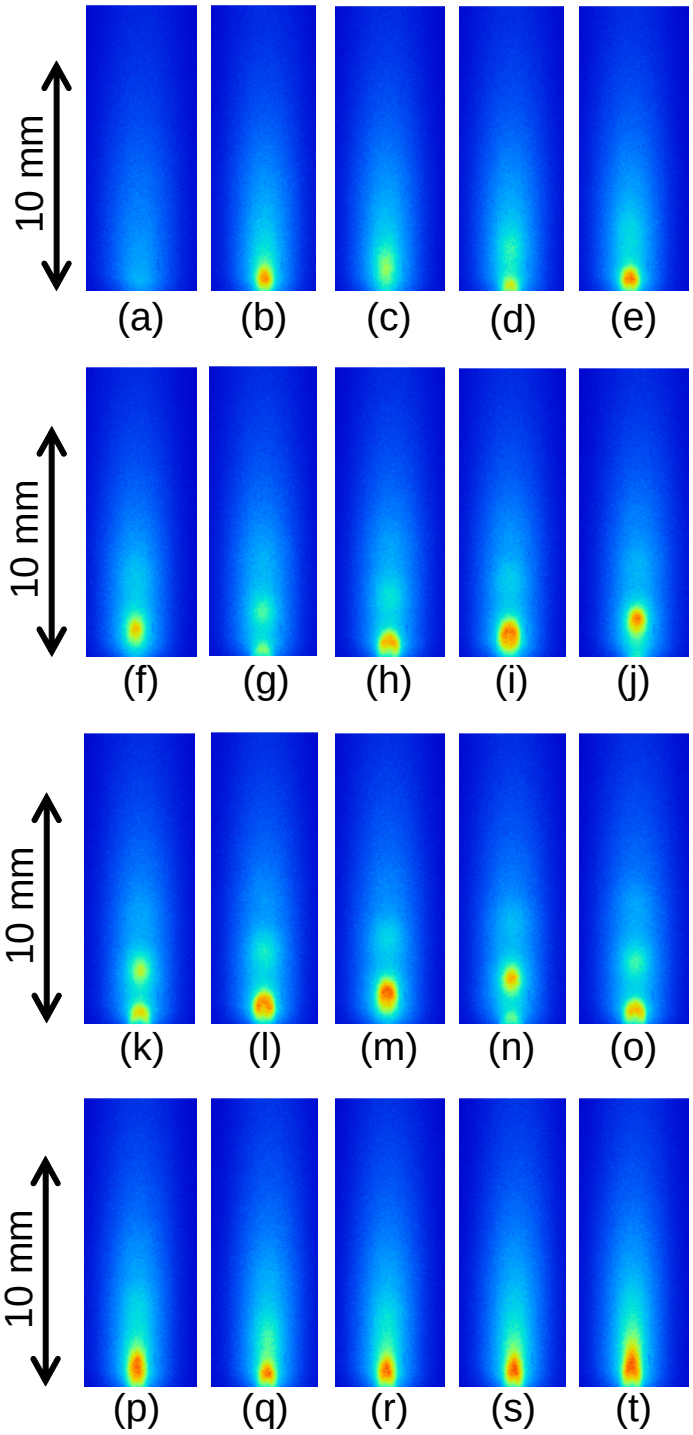

Figure 7. Snap shots of the top part of the flame at delay times of (a) 1, (b) 1.8, (c) 1.825, (d) 1.85, (e) 1.875, (f) 1.9, (g) 1.925 (h) 1.95, (i) 1.975, (j) 2 (k) 2.025, (l) 2.05, (m) 2.075, (n) 2.1 (o) 2.125 (p) 2.6, (q) 2.65, (r) 2.7, (s) 3, and (t) 4 ms after the termination of pulsed microwave power.